Asymmetries of Solar p-mode Line Profiles

Douglas Abrams and Pawan Kumar[1]

Department of Physics

Massachusetts Institute of Technology, Cambridge, MA 02139

Abstract

Recent observations indicate that solar p-mode line profiles are not exactly Lorentzian, but rather exhibit varying amounts of asymmetry about their respective peaks. We analyze p-mode line asymmetry using both a simplified one-dimensional model and a more realistic solar model. We find that the amount of asymmetry exhibited by a given mode depends on the location of the sources exciting the mode, the mode frequency, and weakly on the mode spherical harmonic degree, but not on the particular mechanism or location of the damping. We calculate the dependence of line asymmetry on source location for solar p-modes, and provide physical explanations of our results in terms of the simplified model. A comparison of our results to the observations of line asymmetry in velocity spectra reported by Duvall et al. (1993) for modes of frequency ~ 2.3 mHz suggests that the sources for these modes are located more than 325 km beneath the photosphere. This source depth is greater than that found by Kumar (1994) for acoustic waves of frequency ~ 6 mHz. The difference may indicate that waves of different frequencies are excited at different depths in the convection zone. We find that line asymmetry causes the frequency obtained from a Lorentzian fit to a peak in the power spectrum to differ from the corresponding eigenfrequency by an amount proportional to a dimensionless asymmetry parameter and to the mode linewidth.

Subject headings: Sun — oscillations: sun — p-modes

[1] Alfred P. Sloan Fellow & NSF Young Investigator

1. Introduction

Most previous work in helioseismology has relied on the assumption that solar p-mode line profiles are Lorentzian, which is expected for the power spectrum of randomly forced, damped harmonic oscillators. However, recent results indicate that this may be only approximately true. Duvall et al. (1993) have presented observational evidence from their South Pole data that p-mode line shapes are not exactly Lorentzian, but rather exhibit varying amounts of asymmetry about their respective peaks. This is a difficult observation which has not yet been reproduced by other groups. However, several authors have investigated the problem theoretically, and have found that line profiles are asymmetrical whenever a localized excitation source is present (Gabriel, 1992, 1993, and 1995; Roxbourgh & Vorontsov, 1995; see also Figure 2 of Kumar et al., 1989). Therefore, we believe that the line asymmetry observations of Duvall et al. will be validated when more accurate measurements are available.

The excitation of p-modes is thought to occur in a thin layer near the top of the solar convection zone. All of the previous work on line asymmetry indicates that the degree of asymmetry depends on the depth of the excitation sources. Therefore, p-mode line shapes may provide a means of locating the acoustic sources responsible for exciting modes of various frequencies.

In this paper, we present a detailed analysis of p-mode line profiles for both a simplified one-dimensional model and a realistic solar model, previously used by Kumar et al. (1994) to study peaks in the power spectrum above the acoustic cutoff frequency. For the one dimensional model problem, we analyze the dependence of line asymmetry on source depth, mode dissipation (including linewidth and location of damping), mode frequency, and ℓ; we also investigate the error introduced in p-mode frequency determination by Lorentzian fits to the power spectrum. Our results for the one-dimensional problem are contained in section 2. For the realistic solar model, we investigate the dependence of line asymmetry on source depth, mode frequency and ℓ, and also examine errors in eigenfrequency determination. These results are contained in section 3. We summarize our main conclusions in section 4.

2. Model problem

The following (homogeneous) one-dimensional wave equation describes adiabatic solar oscillations in the Cowling approximation (Deubner and Gough, 1984):

$$\frac{d^2\psi_\omega}{dr^2} + \left[\frac{\omega^2}{c^2} - V(r)\right]\psi_\omega = 0, \tag{1}$$

where $\psi_\omega = \rho^{1/2}c^2\mathrm{div}\vec{\xi_\omega}$, $\vec{\xi_\omega}$ is a Fourier component of the fluid displacement, ρ is the equilibrium density, and c is the sound speed. The effective acoustic potential is given by $V(r) \approx \ell(\ell+1)/r^2 + \omega_{ac}^2/c^2$, where ω_{ac} is the acoustic cutoff frequency. The first term in the potential determines a mode's lower turning point, while the second term peaks near the temperature minimum and causes acoustic waves to be reflected. Solar p-modes can be modelled reasonably well by setting the sound-speed equal to one everywhere and using

the following simple form for the potential (see also Kumar and Lu, 1991; Kumar et al., 1994):

$$V(r) = \begin{cases} \infty & \text{for } r \leq 0, \\ 0 & \text{for } 0 < r < a, \\ \alpha^2 \text{ (constant)} & \text{for } r \geq a, \end{cases} \tag{2}$$

where a is the sound travel time from the lower to the upper turning point of a given mode and α is the acoustic cutoff frequency at the temperature minimum. Waves of angular frequency less than α are trapped below a, while waves of angular frequency greater than α can propagate to infinity; thus, for frequencies less than α there is a discrete spectrum of real eigenfrequencies. Neglecting a weak dependence on mode frequency, different values of a correspond to modes of different degree ℓ.

We now add a damping term and a source term to equation (1). Although the damping processes affecting solar p-modes are quite complex, we assume that for the present purposes they may be modeled by a viscous damping force. Upon adding these two terms, we obtain

$$\frac{d^2\psi_\omega}{dr^2} + i\omega\gamma_\omega(r)\psi_\omega + \left[\omega^2 - V(r)\right]\psi_\omega = f_\omega(r), \tag{3}$$

where $f_\omega(r)$ and $\gamma_\omega(r)$ are the Fourier components of the source function and of the coefficient of the damping term, respectively. As long as the region of excitation is much smaller than the wavelengths considered, we may use $f_\omega(r) = S_\omega\delta(r - r_s)$. Since the source power spectrum S_ω varies negligibly over a typical mode linewidth, it does not affect our calculations of asymmetry and we set it equal to unity for all frequencies. We consider two forms for $\gamma_\omega(r)$. One case we consider is $\gamma_\omega(r) = \Gamma_\omega$ (independent of r), where Γ_ω is the (frequency-dependent) linewidth. The other is $\gamma_\omega(r) = \Gamma'_\omega\delta(r - r_d)$, which is a better approximation to solar p-mode dissipation. These two extreme cases should demonstrate whether or not line asymmetry has any dependence on the details of the damping process.

Equation (3) is easily solved to obtain the power spectrum seen by an observer in the photosphere, and individual peaks in spectra generated in this manner do indeed exhibit varying degrees of asymmetry (see Figure 1). In the next two subsections, we examine the asymmetry when the source is inside or outside the well. In §2c we examine the effects of asymmetry on the accuracy of determining the system's eigenfrequencies using Lorentzian fits to the peaks.

Before proceeding, we introduce a method of quantifying line asymmetry which will be used for the rest of this paper. We decompose the observed power spectrum in the neighborhood of a peak corresponding to a mode α into even and odd functions. Since the odd function is zero at the peak and again far from the peak, its magnitude has a maximum at some intermediate distance from the peak, typically less than one linewidth. The ratio of the maximum magnitude of the odd function to the maximum magnitude of the even function is a dimensionless measure of the asymmetry which we denote by $\eta_\alpha/100$. Then η_α is the percentage line asymmetry of mode α. The sign of η_α is taken to be positive or negative according to whether there is more power on the high- or low-frequency side of the peak, respectively.

2a. Source inside the well

When the source is inside the well and damping is uniform (i.e., $\gamma_\omega(r) = \Gamma_\omega$ everywhere), the solution to equation (3) is given by

$$\psi_\omega(r) = -\left(\frac{\sin kr_s}{k\cos ka + k_1 \sin ka}\right) e^{-k_1(r-a)}, \tag{4}$$

where $k = \sqrt{\omega^2 + i\omega\Gamma_\omega}$ and $k_1 = \sqrt{\alpha^2 - \omega^2 - i\omega\Gamma_\omega}$. When $\Gamma_\omega \ll \omega$ (as is the case for solar p-modes) and $\omega \approx \omega_\alpha$, an eigenfrequency, the velocity power spectrum seen by an observer at location r is given by

$$P_\omega(r) \equiv \omega^2|\psi_\omega(r)|^2 \approx \frac{\omega^2 e^{-2k_1(r-a)}}{(a\alpha)^2}\left[\frac{\sin^2 r_s\omega}{(\Delta\omega)^2 + \Gamma_\omega^2/4}\right], \tag{5}$$

where $\Delta\omega = \omega - \omega_\alpha$. The line-profile depends on the source position through the factor $\sin^2 r_s\omega$ in the numerator. When $\sin r_s\omega_\alpha \approx 1$, the variation of the numerator with frequency over the mode linewidth is small, and the line profile is nearly Lorentzian. (In all cases, the variation over a linewidth of the factor appearing outside the square brackets is negligible.) However, when $\sin r_s\omega_\alpha \approx 0$, the peak is quite asymmetrical. Note that the most asymmetrical peaks, when the source lies inside the well, therefore correspond to modes which are excited to small amplitudes.

For the discussion that follows, it will be useful to rewrite the power spectrum in the neighborhood of a mode frequency as:

$$P_\omega(r) \approx C\left[\frac{\sin^2(\delta + r_s\Delta\omega)}{(\Delta\omega)^2 + \Gamma_\omega^2/4}\right], \tag{6}$$

where C is approximately constant, $\delta = \omega_\alpha(r_s - r_0)$, and r_0 is the closest number to r_s satisfying $\sin r_0\omega_\alpha = 0$. (Note that r_0 may be greater than a; in particular, it need not correspond to a node of the eigenfunction in question.) It is apparent from equation (6) and the discussion above that the asymmetry parameter η_α has the same sign as δ, and that the magnitude of η_α is maximized (*i.e.* peaks are very asymmetrical) when δ is small. When $\delta = 0$, however, the source lies exactly at a node, and it is meaningless to speak of line asymmetry, since the Lorentzian peak is completely suppressed.

We have checked the dependence of line asymmetry on source location, mode frequency, linewidth, and ℓ, when the sources lie within 1000 km (100 seconds of sound travel time) of the upper turning point (see Figure 2). Moving the sources deeper causes η_α to become more positive, except when the source passes through a node, in which case η_α jumps discontinuously from a large positive to a large negative value. This follows from the dependence of δ on r_s: as the source is moved deeper into the well, δ decreases monotonically except when η_α passes through zero, in which case δ jumps discontinuously from $-\pi/2$ to $\pi/2$.

The behavior of the asymmetry as a function of mode frequency depends on the source location: for source locations within 400 km of the upper turning point, the magnitude of η_α is greatest for low-frequency modes, while for some deeper source locations (for

example, 800 km depth), it is greatest for high-frequency modes. (Since the asymmetry for a given mode depends on the locations of its eigenfunction's nodes relative to the source, the modes with the most asymmetrical power spectra continue to change as the source is moved deeper still.)

Increasing the linewidth with other parameters fixed increases the magnitude of the asymmetry, since the variation of the numerator in equation 6 over the extent of the peak is effectively increased. Finally, with the source restricted to lie near the top of the cavity, the magnitude of the asymmetry increases with increasing cavity length (decreasing ℓ value), since the numerator in Equation 6 varies more rapidly.

These dependences of the asymmetry on the linewidth and effective cavity length are quite general and do not depend on the detailed nature of the potential.

We have also considered the case when the damping is localized as a delta function 0-250 km below the upper turning point; we find the dependence of lineshape on the nature and location of damping to be very weak. In order to make meaningful comparisons between the cases of global and local damping, we match the imaginary parts of the respective eigenfrequencies. For cavity lengths corresponding to low degrees ($\ell \approx 5$), we consider linewidths of up to 15 μHz, while for cavity lengths corresponding to higher degrees, we consider larger linewidths; for $\ell \gtrsim 350$, we consider linewidths of up to 50 μHz. In this parameter regime, we find that if $1\% \lesssim |\eta_\alpha| \lesssim 10\%$, changing the damping location changes η_α by less than 10% of its total value; we also find that results are similar to those obtained using uniform damping [1].

Thus, when the source lies just beneath the upper turning point, lineshapes depend strongly on source location, mode frequency, linewidth, and ℓ, but only weakly on the type and location of damping. Placing the source in the evanescent region leads to similar conclusions; that case is discussed next.

2b. Source outside the well

When damping is uniform throughout the well, the solution of equation (3) for the amplitude seen by an observer at location r, due to a point source at r_s ($r > r_s > a$), is given by:

$$\psi_\omega(r) = \left[\frac{2k\cos ka \sinh k_1(r_s-a) + 2k_1 \sin ka \cosh k_1(r_s-a)}{k\cos ka + k_1 \sin ka}\right] \frac{e^{-k_1(r-a)}}{2k_1}, \tag{7}$$

where k and k_1 are defined as before. However, we gain more insight in this case by considering separately the contributions to the total amplitude due to waves which travel along different paths from the source to the observer. (This is the approach taken by Duvall

[1] Other damping schemes yield similar results as well; in particular, when the damping is non-zero above a certain depth (near the upper turning point), or when it is nonzero only in a finite range at the top of the well, the behavior of the asymmetry is essentially unchanged.

et al., 1993.) In particular, the total observed amplitude is given by the sum of three parts: (1) the wave which travels directly outward from the source to the observer (hereafter the direct wave), (2) the wave which first travels toward the cavity and is reflected back toward the observer at the potential step (hereafter the reflected wave), and (3) the sum of the infinite sequence of waves which arises due to multiple reflections in the cavity (hereafter the cavity wave).

The total amplitude seen by an observer is thus given by:

$$\psi_{\omega,tot}(r) = \psi_{\omega,dir}(r) + \psi_{\omega,ref}(r) + \psi_{\omega,cav}(r) = \frac{-e^{-k_1(r-r_s)}}{2k_1}$$

$$-\frac{e^{-k_1(r+r_s-2a)}}{2k_1}\left(\frac{k_1+ik}{k_1-ik}\right) + \frac{e^{-k_1(r+r_s-2a)+2ika}k}{2kk_1+i(k_1^2-k^2)} \cdot \left[1+e^{2ika}\left(\frac{ik+k_1}{ik-k_1}\right)\right]^{-1}. \qquad (8)$$

The first two terms are roughly constant in magnitude and phase over a typical linewidth (up to 50 μHz), while the third term (the cavity wave) exhibits resonance behavior. In particular, constructive interference occurs when the waves due to multiple reflections in the cavity arrive at the observer in phase; the frequencies at which this occurs are the eigenfrequencies. Therefore, for all cases of interest, the amplitude of the cavity wave is much greater than the amplitudes of the direct and reflected waves at an eigenfrequency. The magnitude of the cavity wave in the neighborhood of a mode eigenfrequency varies symmetrically about the peak. However, interference between the cavity wave and the sum of the direct and reflected waves causes the total power seen by an observer to be asymmetric about the peak.

For small linewidths (specifically, in the limit that k and k_1 are real), the cavity wave leads the direct wave by $\pi/2$ in phase when ω is equal to an eigenfrequency; this phase difference is due to the phase shifts experienced by a wave upon entering or leaving the well, plus the phase shift due to travel from the top of the cavity to the bottom and back, with an inverting reflection at the bottom. Since the reflected wave is smaller in magnitude than the direct wave, it follows that at resonance, the cavity wave always leads the sum of the direct and reflected waves in phase. Furthermore, the phase of the cavity wave is a monotonically increasing function of frequency. Thus the observed asymmetry is always negative, while the magnitude of asymmetry depends on the differences in amplitude and phase between the three interfering terms. (It suffices to evaluate these at the source location, since the three waves experience the same phase change and attenuation in traveling from the source to the observer.) The relative amplitudes and phases of the three waves near a mode frequency are shown in Figure 3. These conclusions are unaltered by the presence of damping.

We have investigated the dependence of the asymmetry on source location, mode frequency, mode degree, and linewidth (see Figure 2). Moving the source away from the cavity leads to more asymmetrical line profiles because the amplitude of the cavity wave (evaluated at the source location) decreases due to attenuation in the evanescent zone, while the amplitude of the direct wave is unaffected; the interference of the direct wave with the cavity wave therefore has a more pronounced effect. Increasing mode frequency while

keeping the linewidth fixed, on the other hand, leads to less asymmetrical profiles because the amplitude of the cavity wave at resonance *increases* with increasing mode frequency, relative to the sum of the direct and reflected waves. We find that increasing the cavity length (decreasing ℓ) while keeping the linewidth fixed yields more asymmetrical profiles. Finally, increasing the linewidth yields more asymmetrical line profiles, since increasing the damping decreases the amplitude of the cavity wave without significantly affecting the amplitudes of the direct or reflected waves.

As in the case when the source is inside the well, line profiles depend very weakly on the nature and location of damping: the numbers quoted in this respect in §2a apply here as well.

We have shown that line asymmetry, when the source is above or below the upper turning point, depends strongly on source location, linewidth, mode frequency, and ℓ, but only weakly on the nature and location of damping. Line asymmetry also leads to errors in determining the system's eigenfrequencies using Lorentzian fits to the peaks; that is discussed next.

2c. Errors in eigenfrequency determination

Errors in eigenfrequency determination by Lorentzian fits to observed power spectra occur for two reasons. First of all, the observed peak in a given line profile may be shifted from the corresponding eigenfrequency. Secondly, the frequency of best fit may differ from the frequency corresponding to the observed peak. We have tested eigenfrequency determination error in the model problem by fitting Lorentzians to profiles generated for different source locations, mode frequencies, cavity lengths, and linewidths, including cases when the source is inside or outside the well and when the damping is global or local.

We find a simple relationship between percent asymmetry and the amount $\delta\nu_\alpha$ by which the frequency obtained from a Lorentzian fit to the power spectrum of a mode α differs from the corresponding eigenfrequency. Expressed as a percentage of the corresponding linewidth (Γ_α), $\delta\nu_\alpha$ is proportional to the percentage asymmetry, η_α:

$$\delta\nu_\alpha = \left[\frac{b}{100}\right]\Gamma_\alpha\eta_\alpha, \tag{9}$$

where b, the constant of proportanality, depends only on the type of damping used, and not on mode frequency, linewidth, ℓ value, or source location. For spectra generated with global damping, $b \approx 1.6$, whereas for spectra generated with local damping, $b \approx 1.1$. (See Figure 5 of §3c).

3. Line asymmetry for p-modes of the Sun

We have also analyzed line asymmetry using a solar model due to Christensen-Daalsgard (1991). Our calculations of p-mode power spectra include radiative damping and stochastic mode excitation due to turbulent convection, but ignore dissipation due to the interaction of modes with turbulent convection. Based on the calculations described in §2, we do not expect our results to depend on the type of damping used; however, due

to the fact that the linewidths we calculate are smaller than the observed linewidths, we must interpret our numerical results taking into account the dependence of asymmetry on linewidth found for the simple model of §2.

Theoretical power spectra are computed by solving for Green functions of the nonadiabatic oscillation equations in the Cowling approximation. The details of this calculation are given by Kumar (1994). As described therein, the mean velocity power spectrum due to stochastic excitation by turbulent convection is given by:

$$\langle P_\omega \rangle \approx \frac{\omega^2}{{R_\odot}^2} \int dr \int dr_0 \left| \rho(r_0) \frac{d}{dr_0} G_\omega(r; r_0) \right|^2 S_\omega(r_0), \tag{10}$$

where $G_\omega(r; r_0)$ is the Green function for a source term in the momentum equation, and $S_\omega(r_0)$ is the source strength, which we consider to be the Reynold's stress. The outer integral is over the region in the photosphere where the optical line is formed, and the inner integral is over the source region. The p-mode power spectrum calculated using the above equation depends on the derivative of the Green function because we consider only quadrupole sources of sound waves, which correspond to the derivative of the Reynold's stress; this derivative is transferred to the Green function after integration by parts. The power spectrum for dipole sources, obtained using equation (10) with G_ω in place of dG_ω/dr, yields different lineshapes.

The source strength for quadrupole acoustic emission is given by Kumar (1994):

$$S_\omega(r_0) \sim \frac{H^4 v_H^3}{1 + (\tau_H \omega)^{7.5}}, \tag{11}$$

where H, τ_H, and v_H are, respectively, the correlation lengths ("mixing lengths") , correlation times, and velocities of energy bearing convective eddies at radius r_0 ($v_H \approx H/\tau_H$). Due to its strong dependence on convective velocity, the source strength is expected to be a sharply peaked function of position (see Figure 1 of Kumar, 1994). We treat the unknown source strength as a Gaussian of width 50 km (this is roughly what is expected if we take the convective velocity as given by standard mixing length theory), and vary its peak position within the top 1200 km of the convection zone. We compute the p-mode line profiles and asymmetries which, when compared with observations, should yield the radial location of the acoustic sources. We note that the equilibrium solar model was calculated using standard mixing length theory.

In the next two subsections, we present the results of our solar model calculations for the dependence of line asymmetry on source location, mode frequency, and mode degree, and explain our results in terms of the simplified model. In §3c we discuss errors in eigenfrequency determination introduced by line asymmetry.

3a. Solar model results

We have calculated solar p-mode power spectra for ℓ between 5 and 500, frequencies in the range $\sim 1 - 5$ mHz, and source locations in the top 1200 km of the convection

zone. Peaks exhibit varying amounts of asymmetry, depending on source location, mode frequency, and mode degree (see Figure 4).

Moving the sources deeper causes the asymmetry parameter η_α to become more positive, unless the source passes through a node, in which case η_α jumps from a large positive to a large negative value. (There is some deviation from this pattern when the sources lie in the top 30 km of the convection zone.)

When the source depth is less than 400 km, the most asymmetrical peaks (with $|\eta_\alpha| \approx 10\%$) correspond to low-frequency modes, while peaks corresponding to modes above 3 mHz show very little asymmetry ($|\eta_\alpha| < 4\%$). The asymmetry for mode frequencies below 3 mHz is negative, *i.e.* there is more power on the lower frequency side of the peak. In contrast, for some deeper source locations (for example, depths between 800 and 1000 km), the most asymmetrical peaks correspond to high-frequency modes, while peaks corresponding to modes below 3 mHz show little asymmetry. In this case, the asymmetry of the most asymmetrical peaks is positive. In general, which modes have the most asymmetrical power spectra, and the sign of the corresponding asymmetries, depends on the location of the sources, and changes as the sources are moved deeper still.

For any source location and mode frequency, the magnitude of the asymmetry is a weakly increasing function of ℓ; η_α changes by no more than a few percentage points over the range $\ell = 5 - 500$.

Duvall et al. (1993) found negative asymmetry in p-mode velocity spectra corresponding to modes of frequency 2.2-2.5 mHz and degrees in the range 157-221; from their data we find that $\eta_\alpha = -2.5\%$ for these modes. Allowing an uncertainty in η_α of $^+/_-$ 0.5%, our numerical calculations reproduce this result provided we assume that the sources for modes of this frequency lie at a depth of 325-525 km beneath the photosphere. However, our calculated linewidths are less than the observed linewidths in this frequency range, which implies that for any source location, we underestimate the magnitude of η_α. Since $|\eta_\alpha|$ for these modes is a decreasing function of source depth for source locations within the top few scale heights of the convection zone, this technique therefore yields a lower bound on the source depth for these modes of 325 km.

Duvall et al. found *positive* line asymmetry in the intensity power spectra of the same modes. This is a puzzling result. At any given location in the solar atmosphere, the dynamical oscillation equations may be solved for the pressure and density perturbations (δp and $\delta\rho$) in terms of the radial displacement function (ξ_r), the radial wave number, and equilibrium properties of the atmosphere. In the model problem of §2, it can be shown analytically that ξ_r is the only one of these quantities which varies appreciably over a mode linewidth, and numerical calculations show this to be the case for the solar model. As a result we find that the perturbation to any thermodynamic quantity is essentially proportional to the radial displacement function. Any reversal of asymmetry must therefore be due to a subtle detail of the process by which the observed flux is modulated by pulsation.

3b. Explanation of solar model results

The behavior described above is in qualitative agreement with the results obtained

using the simplified model of §2, except for the dependence of asymmetry on source position when the sources lie in the top 30 km of the convection zone. This disagreement is most likely due to the more complicated behavior of the solar potential at the top of the convection zone. However, for the extremely limited range of source locations involved, the variation in asymmetry due to different source locations is correspondingly small - less than 15% of the total asymmetry.

In the simple model problem, the asymmetry depends strongly on the cavity length (the effective mode degree), while in the solar model the asymmetry is a very weak function of degree. The difference is accounted for by the increase of linewidth with degree in the solar model, which cancels the effect on the asymmetry of decreasing the effective cavity length. (The dependence of linewidth on ℓ calculated using the solar model is similar to the observed dependence; therefore, we do not expect this result to be affected significantly by the discrepancies between calculated and observed linewidths mentioned earlier.)

As mentioned previously, the derivative used in calculating power spectra from the solar model has an important effect on the shapes of lines in the spectra (see equation 10). In calculating power spectra using the simple model of §2, no derivative is explicitly used. However, the dependent variable used there is $\psi = \rho^{1/2}c^2\mathrm{div}\vec{\xi}$, which is approximately equal to $\rho^{1/2}c^2 d\xi_r/dr$ near the surface. Due to the derivative present in the definition of ψ, the shapes of lines in spectra calculated using the simple model agree qualitatively with the shapes of lines in spectra calculated using the solar model. (Note that the choice of variables determines the form of the acoustic potential. For the set of variables used here, the effective potential for p-modes may be approximated by the square-well potential of equation 2; for other sets of variables not involving derivatives - for example, the set used by Gabriel, 1992, and Roxbourgh & Vorontsov, 1995 - the acoustic potential bears little resemblance to the square-well potential.)

3c. Errors in eigenfrequency determination

As in the one-dimensional model problem, we find that for a mode α, the frequency shift $\delta\nu_\alpha$ (see §2c), expressed as a percentage of the linewidth Γ_α, is proportional to the percentage asymmetry, η_α. (See Figure 5). The constant of proportionality b, defined by equation (9), is found to be 1.5 in the solar case. The linear relationship holds regardless of source location, mode frequency, or mode degree, as in the one-dimensional problem.

4. Summary and discussion

The shapes of lines in p-mode power spectra are, in general, not symmetric about the peak. We find that the magnitude and sense of asymmetry depend strongly on the location of the sources and on mode frequency, and weakly on mode degree (ℓ).

We define a dimensionless measure of asymmetry for a given mode by decomposing its power spectrum in the neighborhood of the peak into even and odd components; the ratio of the peak amplitudes of the two components, expressed as a percentage, measures the magnitude of the asymmetry. We define the asymmetry to be positive (or negative) when there is more power on the high-frequency (or low-frequency) side of the peak.

We have calculated the line asymmetry for p-modes of a simplified one-dimensional

problem, as well as a solar model, for various source locations. Line asymmetry is found to have similar behavior in both cases. In particular, we find that moving the sources deeper causes the asymmetry to become more positive, unless the source passes through a node of the mode eigenfunction, in which case the asymmetry changes discontinuously from a large positive to a large negative value. The magnitude of the asymmetry increases weakly with mode degree: for fixed source location and approximately constant mode frequency, the absolute value of the asymmetry parameter increases by no more than a few percentage points over the range $\ell = 5$ to 500. For the one-dimensional problem, the asymmetry has no significant dependence on the location or nature of damping as long as mode linewidth is held fixed.

Physically, line asymmetry may be understood in terms of a wave-interference model, in which waves travel along different paths from the source to the observer, as suggested by Duvall et al. (1993). However, we find that the line asymmetry does not depend significantly on phase shifts due to nonadiabatic effects in evanescent regions, as Duvall et al. suggested.

By comparing the asymmetries of theoretically calculated profiles to the asymmetries of the profiles observed by Duvall et al. (1993) for modes of frequency ~ 2.3 mHz, we set a lower bound on the source depth for these modes of 325 km (measured with respect to the bottom of the photosphere). This is greater than the depth of 140 $^{+}/_{-}$ 60 km found by Kumar (1994) for the sources exciting acoustic waves above the acoustic cutoff frequency (~ 5.3 mHz). Based on the theory of wave generation by turbulent convection and standard mixing length theory, we expect the emission of acoustic waves to occur deeper in the convection zone for waves of lower frequency. The difference between the present results and the results of Kumar (1994) may be a confirmation of this prediction.

We find that line asymmetry causes the frequency obtained from a Lorentzian fit to a given peak in the power spectrum to differ from the corresponding eigenfrequency by an amount proportional to the mode linewidth and to the asymmetry of the peak. This holds for both the square-well potential model and the more realistic solar model. As a percentage of the linewidth, this frequency shift for the solar model is about 1.5 times the percent asymmetry of the peak.

Duvall et al. reported that the sense of line asymmetry is different in velocity and intensity power spectra; in particular, for modes of frequency below 3 mHz, they found negative asymmetry in velocity spectra and positive asymmetry in intensity spectra. This is a puzzling result for which we have no explanation.

Acknowledgements: We thank Tom Duvall for sending us the data used in §3a, and Eliot Quataert for many useful comments and discussions. This work was supported by NASA grant NAGW-3936.

REFERENCES

Duvall, T.L.Jr., Jefferies, S.M., Harvey, J.W., Osaki, Y., and Pomerantz, M.A. 1993, ApJ, 410, 829

Gabriel, M. 1992, AA, 265, 771

Gabriel, M. 1993, AA, 274, 935

Gabriel, M. 1995, AA, 299, 245

Goldreich, P. and Keeley, D.K. 1977, ApJ, 212, 243

Goldreich, P. & Kumar, P. 1990, ApJ, 363, 694

Goldreich, P., Murray, N., & Kumar, P. 1993, ApJ, 424, 466

Kumar, P., & Lu, E. 1991, ApJ, 375, L35

Kumar, P. 1994 ApJ, 428, 827

Kumar, P, Fardal, M.A., Jefferies, S.M., Duvall, T.L. Jr., Harvey J.W., and Pomerantz, M.A. 1994, ApJ, 422, L29

Roxbourgh, I.W. & Vorontsov, S.V., 1995, MNRAS, 272, 850

FIGURE CAPTIONS

FIG 1 Two peaks with values of the asymmetry parameter η_α of -5% and -10%; see the text for the definition of η_α. Both spectra were calculated using the 1-D model with $a = 3275$ seconds of sound travel time and $\nu = 1.5$ mHz. For the peak with $\eta_\alpha = -10\%$, the source was placed at the upper turning point; for the other, the source was placed 300 km below the upper turning point. Line profiles with the same value of the asymmetry parameter η_α look essentially identical, regardless of source location, frequency, cavity length, linewidth, or type of damping.

FIG 2 a) Asymmetry in the 1-D model (quantified in terms of the parameter η_α) as a function of source height above the upper turning point (h) for modes in cavities of approximate length 3275s, 1625s, and 500s. (Cavity lengths are measured in terms of sound travel time.) Points where η_α abruptly changes from positive to negative (with decreasing h) correspond to nodes of the respective eigenfunctions. Linewidth was fixed at 5 μHz for all of these calculations. b) Also shown is asymmetry in the 1-D model as a function of linewidth for modes in cavities of length 3275s and 475s. Mode frequency was fixed at 3.0 mHz for these calculations.

FIG 3 Plotted on the same set of axes are: i) The ratio of the amplitude of the cavity wave to the amplitude of the direct wave (this ratio varies symmetrically about its peak), ii) The phase of the cavity wave with respect to the direct wave (in radians), and iii) The ratio of the amplitude of the reflected wave to the amplitude of the direct wave. (All three curves were calculated using the 1-D model, with the source outside the cavity, for a peak with $\eta_\alpha = -10\%$.)

FIG 4 Asymmetry in the solar model (quantified in terms of the parameter η_α) as a function of source depth (measured relative to the top of the convection zone) for modes with $\ell \approx 5$, 100, 250, and 375. Points where η_α changes abruptly from positive to negative (with increasing depth) correspond to nodes of the respective eigenfunctions.

FIG 5 Frequency shifts (expressed as percentages of corresponding linewidths) of best-fit frequencies from eigenfrequencies, versus percentage asymmetry η_α. These points correspond to the peaks, calculated using the solar model, whose asymmetries are plotted in Figure 4. The slope of the line is approximately 1.5.

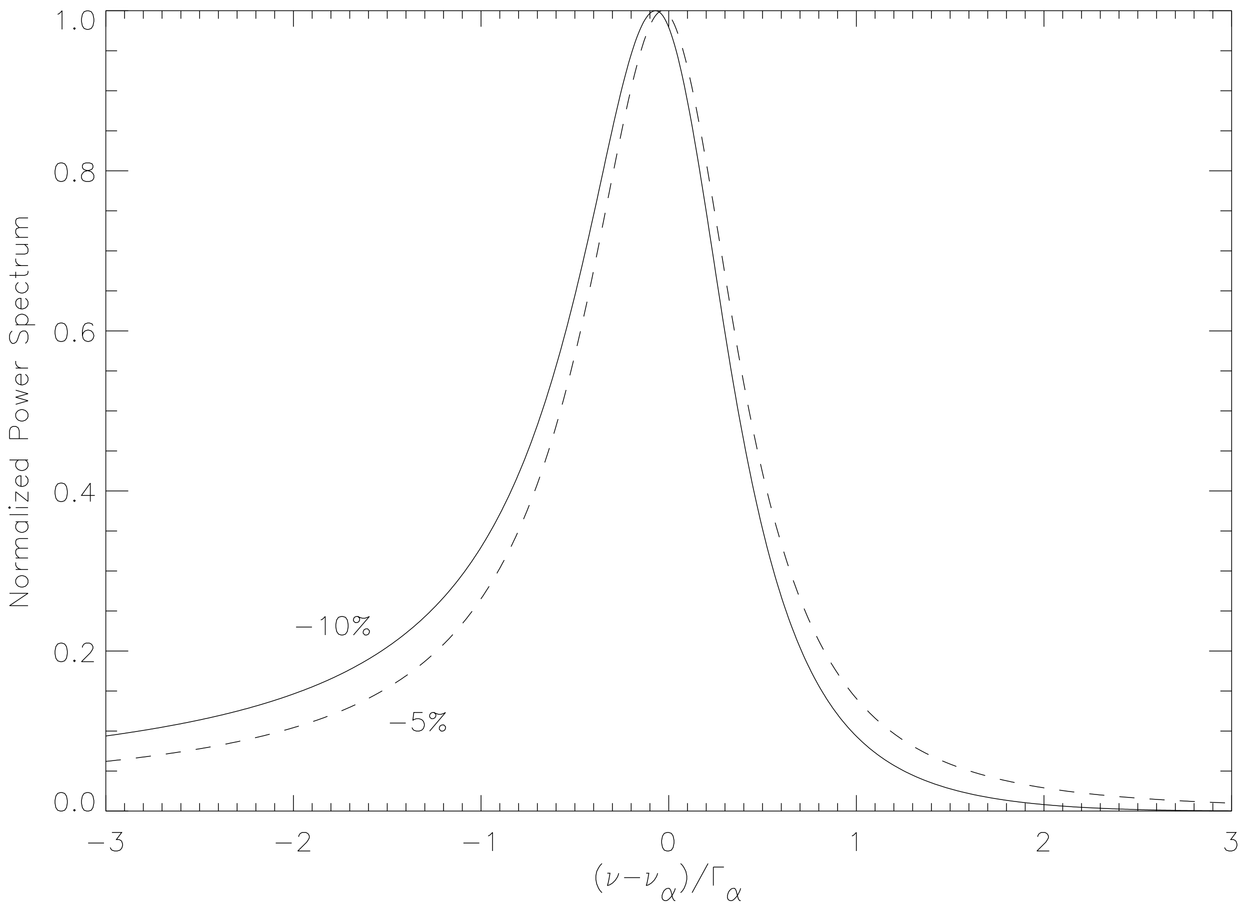

1.0
0.8
0.6
0.4
0.2
0.0
Normalized Power Spectrum
−10%
−5%
−3
−2
−1
0
1
2
3
$(\nu-\nu_\alpha)/\Gamma_\alpha$

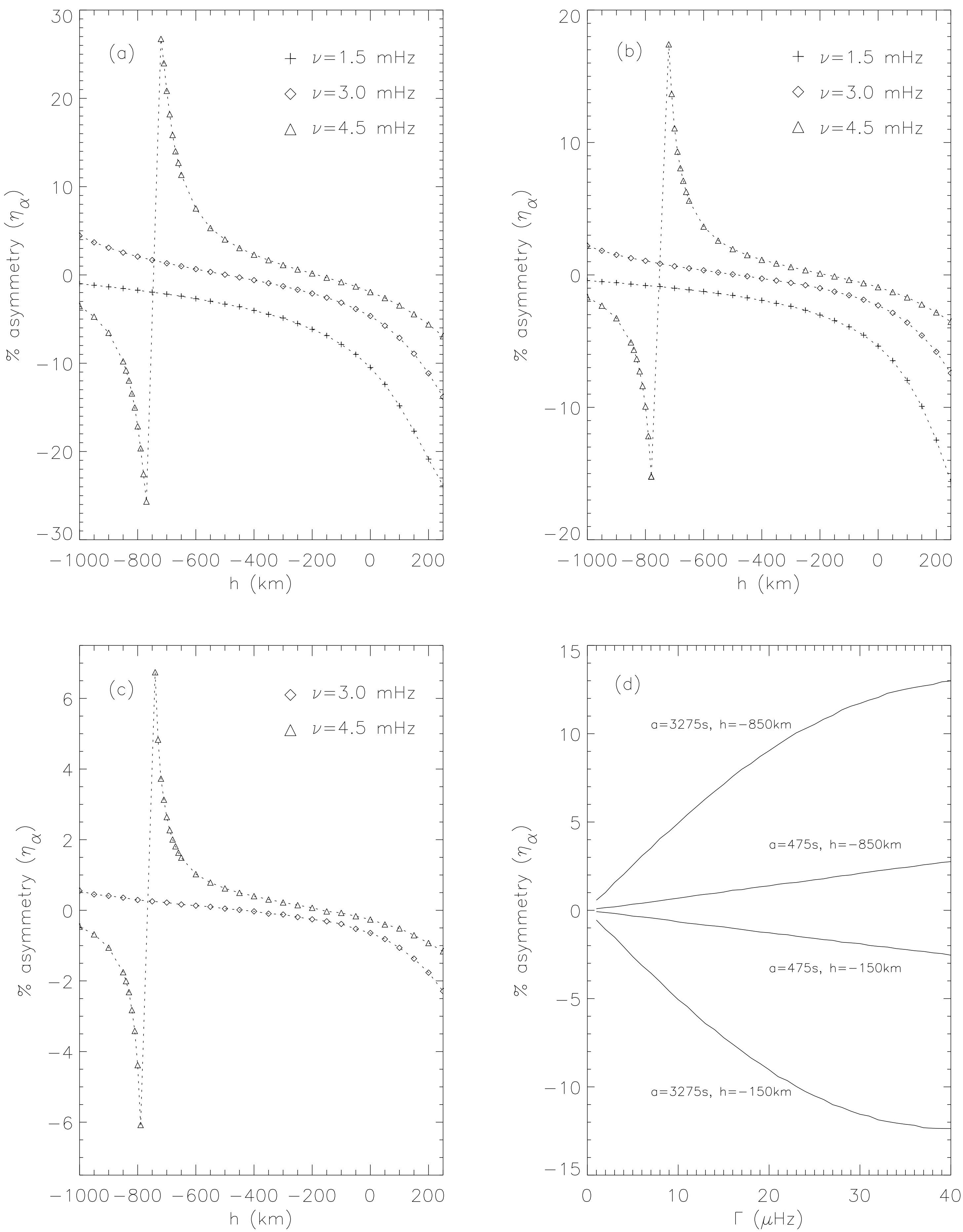
(a)
ν=1.5 mHz
ν=3.0 mHz
ν=4.5 mHz
% asymmetry (η_α)
h (km)
(b)
ν=1.5 mHz
ν=3.0 mHz
ν=4.5 mHz
% asymmetry (η_α)
h (km)
(c)
ν=3.0 mHz
ν=4.5 mHz
% asymmetry (η_α)
h (km)
(d)
a=3275s, h=−850km
a=475s, h=−850km
a=475s, h=−150km
a=3275s, h=−150km
% asymmetry (η_α)
Γ (μHz)

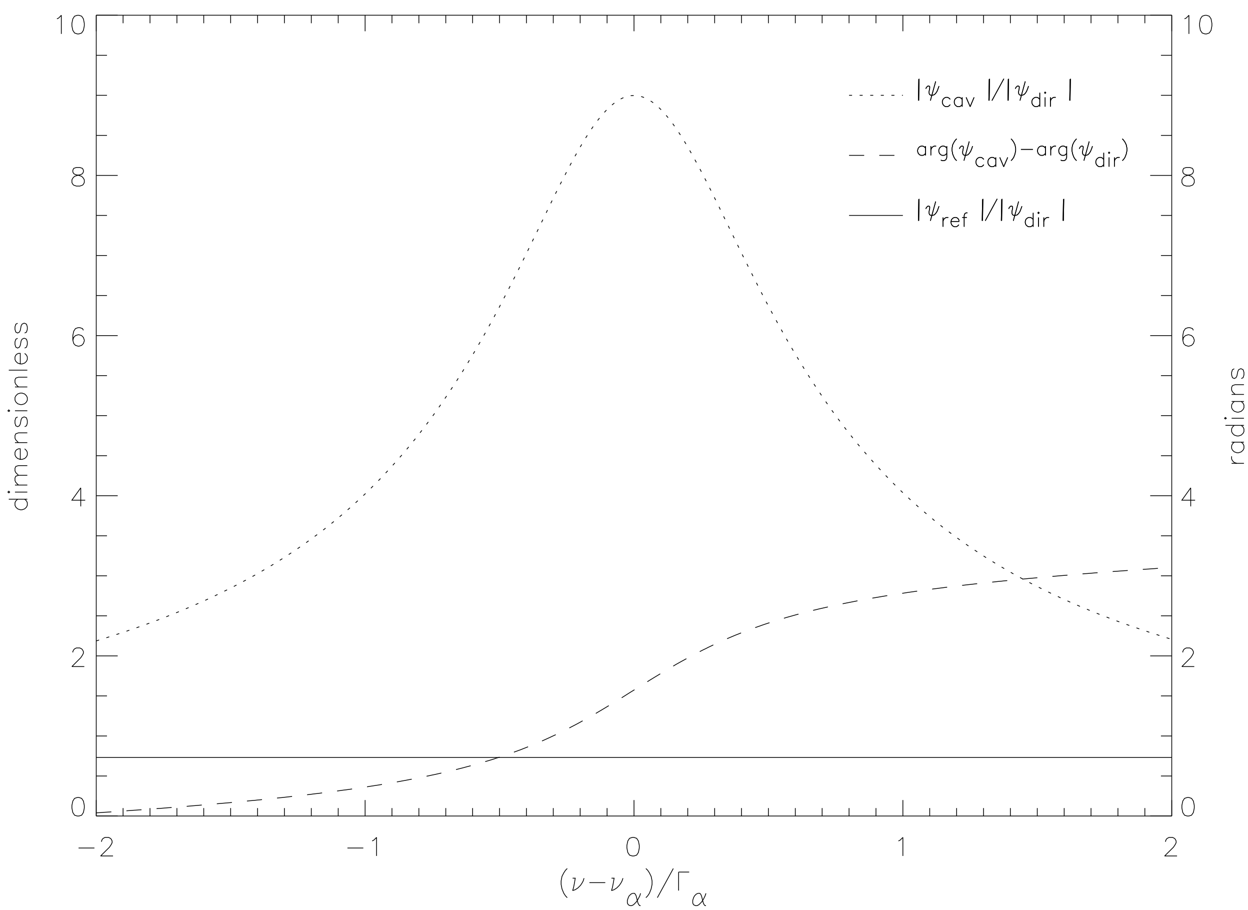

10
8
6
4
2
0
dimensionless
radians
$|\psi_{cav}|/|\psi_{dir}|$
$\arg(\psi_{cav})-\arg(\psi_{dir})$
$|\psi_{ref}|/|\psi_{dir}|$
−2
−1
0
1
2
$(\nu-\nu_\alpha)/\Gamma_\alpha$

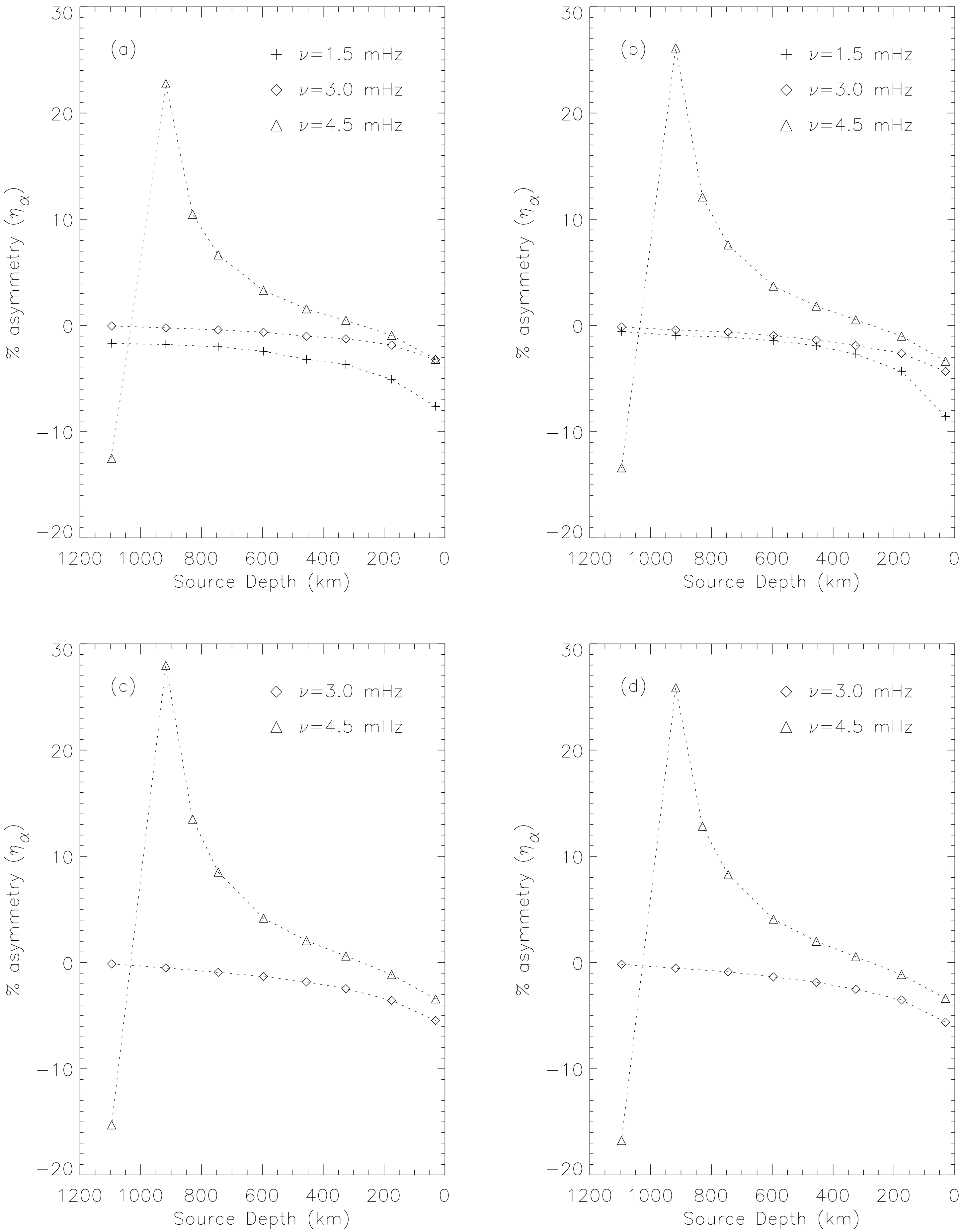

(a)
ν=1.5 mHz
ν=3.0 mHz
ν=4.5 mHz
% asymmetry (η_α)
Source Depth (km)
(b)
ν=1.5 mHz
ν=3.0 mHz
ν=4.5 mHz
% asymmetry (η_α)
Source Depth (km)
(c)
ν=3.0 mHz
ν=4.5 mHz
% asymmetry (η_α)
Source Depth (km)
(d)
ν=3.0 mHz
ν=4.5 mHz
% asymmetry (η_α)
Source Depth (km)

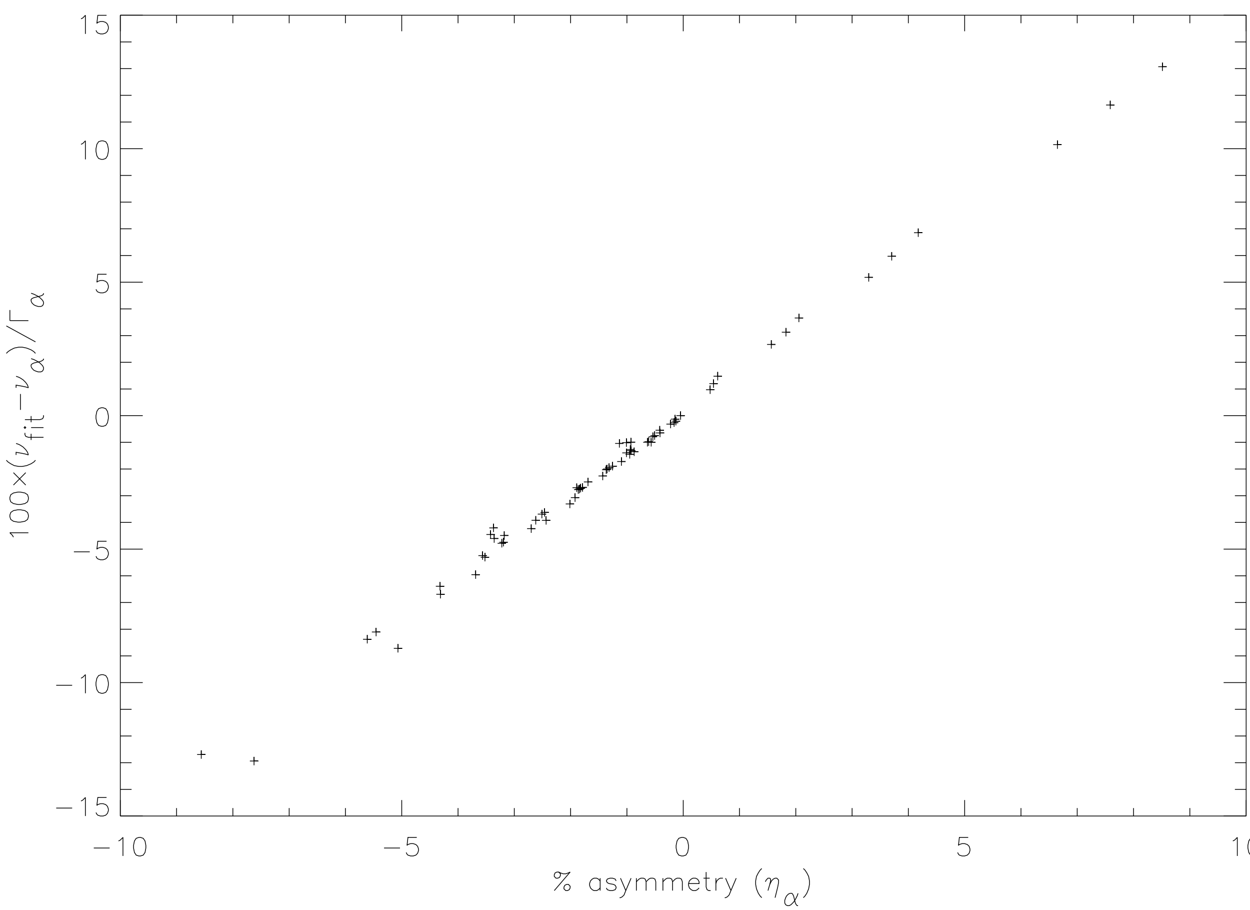
15
10
5
0
−5
−10
−15
−10
−5
0
5
10
$100\times(\nu_{\rm fit}-\nu_\alpha)/\Gamma_\alpha$
% asymmetry (η_α)